Multiscale Modeling of an 8-Week Combination Regimen of Bemnifosbuvir and Ruzasvir in Patients with Chronic Hepatitis C Virus Infection

Carolin Zitzmann[1], Ruy M. Ribeiro[1], Aurelien Marc[1,3], Xiao-Jian Zhou[2] and Alan S. Perelson[1,*]

Bemnifosbuvir (BEM) and ruzasvir (RZR) are pan-genotypic HCV polymerase (NS5B) and NS5A inhibitors, respectively. In a single-arm study (NCT05904470), 215 treatment-naïve, adherent participants with chronic HCV (with or without cirrhosis) received BEM 550 mg QD plus RZR 180 mg QD for 8 weeks. We employed a multiscale mathematical model fitted to the HCV RNA and ALT dynamics to quantify the antiviral activity and evaluate the modes of action of BEM and RZR. We found that after treatment initiation, the viral load (VL) decreased in a triphasic manner, with a very rapid first phase lasting <12 h. The population estimate of the time to reach the LLOQ (VL ≤ 15 IU/mL) was 11 days for individuals in fibrosis stages F0–F3 and 15.6 days for those in F4, while the estimate of the time to reach a hypothetical cure boundary (VL ≤ 6.7×10^{-4} IU/mL) was 6.5 weeks for F0–F3 and 6.9 weeks for F4, with some variability between individuals. The population estimate of the effectiveness of the 8 weeks of treatment in blocking viral replication was 98.6% for F0–F3 and 99.4% for F4, while the estimate of the effectiveness in blocking viral assembly/secretion was 99.8% for F0–F3 and 99.0% for F4. We also found a treatment-induced 70% enhancement of the rate of intracellular HCV RNA degradation. The estimated efficacy of therapy was similar across genotypes 1 to 4. Thus, our modeling supports the conclusions that BEM/RZR is pan-genotypic, has high antiviral effectiveness and leads to rapid viral clearance in both cirrhotic and non-cirrhotic patients.

Study Highlights

WHAT IS THE CURRENT KNOWLEDGE ON THE TOPIC?

☑ Direct-acting antivirals cure >95% of HCV infections, but treatment gaps remain, especially in patients with genotype 3 infection or cirrhosis. Bemnifosbuvir/ruzasvir (BEM/RZR) is a potent pan-genotypic regimen that achieved a 98% SVR rate in compliant patients in a phase II trial, but its within-host mechanisms of viral suppression are not fully defined.

WHAT QUESTION DID THIS STUDY ADDRESS?

☑ This study examined which viral kinetic mechanisms explain the rapid HCV RNA decline during BEM/RZR therapy and whether these effects differ by genotype or fibrosis stage.

WHAT DOES THIS STUDY ADD TO OUR KNOWLEDGE?

☑ A multiscale viral dynamics model fit to longitudinal HCV RNA and ALT data showed that viral decline is best explained by three complementary effects: inhibition of intracellular HCV RNA production, inhibition of virion assembly/secretion, and enhanced intracellular HCV RNA degradation. The model captured the rapid early viral suppression and predicted consistently high antiviral activity, including in genotype 3 and cirrhotic patients.

HOW MIGHT THIS CHANGE CLINICAL PHARMACOLOGY OR TRANSLATIONAL SCIENCE?

☑ These findings provide a mechanistic rationale for the high cure rates observed with BEM/RZR and support multiscale viral kinetic modeling as a translational tool to optimize HCV regimens and evaluate shorter treatment strategies.

Hepatitis C virus (HCV) infection remains a major global public health concern, affecting millions worldwide and contributing to significant liver-related disease and death. The introduction of direct-acting antivirals (DAAs) marked a turning point in HCV treatment.[1] These therapies, which directly target essential viral proteins, have largely replaced earlier interferon (IFN)-based

[1]Theoretical Biology and Biophysics, Los Alamos National Laboratory, Los Alamos, New Mexico, USA; [2]Atea Pharmaceuticals, Inc., Boston, Massachusetts, USA; [3]Present address: Immunology of Viral, Auto-immune, Hematological and Bacterial Diseases (IMVA-HB/IDMIT Department), Université Paris-Saclay, CEA, INSERM, UMR1184, Fontenay-aux-Roses/Le Kremlin-Bicêtre, France. *Correspondence: Alan S. Perelson (asp@lanl.gov)

Received May 21, 2026; accepted August 12, 2026. doi:10.1002/cpt.70454

regimens,[2] which required at least 48 weeks of treatment and achieved only modest efficacy. Furthermore, IFN-based treatments were poorly tolerated, triggering significant systemic side effects due to their broad and nonspecific activation of the immune system.[3–5]

DAAs specifically inhibit essential viral proteins, including NS5A (a multifunctional phosphoprotein critical for viral replication and assembly), NS5B (the RNA-dependent RNA polymerase), and NS3/4A (a serine protease), thereby significantly reducing viral replication and enhancing therapeutic outcomes. Although DAAs are highly effective, treatment failures still occur, and certain patient populations are more difficult to treat than others.

Several factors contribute to non-response or viral relapse, including the presence of resistance-associated substitutions (RASs), prior treatment history, advanced fibrosis or cirrhosis, high baseline viral load, and poor adherence.[6–8] Genotype (GT) 3, which represents 22–30% of all HCV infections, remains more difficult to treat than other HCV GTs, particularly in patients with cirrhosis, due to its association with faster disease progression, virus-induced steatosis, and a higher prevalence of RASs.[9] The presence of baseline NS5A RASs, such as Y93H and A30K, can significantly reduce response to NS5A inhibitors, especially in cirrhotic individuals. As a result, GT 3 cirrhotic patients often require longer treatment durations or intensified regimens to achieve SVR.[10] Thus, better pan-genotypic regimens with high resistance barriers and high effectiveness in both cirrhotic and non-cirrhotic patients and GT3 patients are still needed.

Bemnifosbuvir (BEM) and ruzasvir (RZR) represent a promising new two-drug combination treatment for managing chronic hepatitis C.[11–14] BEM inhibits the HCV NS5B protein, leading to chain termination, and it demonstrated potent pan-genotypic activity *in vitro*, exceeding the potency of sofosbuvir, a frequently used HCV polymerase inhibitor, by 10-fold.[15] RZR, formerly known as MK-8408, is a pan-genotypic HCV NS5A inhibitor targeting this multifunctional viral phosphoprotein essential for HCV replication complex assembly, virion assembly, and secretion.[16] NS5A inhibitors are known for their rapid antiviral action and high potency, but RASs in the NS5A region can reduce efficacy. RZR has demonstrated *in vitro* activity against common NS5A RASs, suggesting it may retain effectiveness in some treatment-experienced populations where other NS5A inhibitors fail.[16,17]

The combination of BEM and RZR has shown high potency *in vitro* and favorable pharmacokinetics, allowing for once-daily oral dosing.[13] In a recent phase II trial (NCT05904470[18]), 8 weeks of treatment with BEM and RZR led to a sustained virologic response at 12 weeks post-treatment (SVR12) in 98% of treatment-adherent patients, including those with compensated cirrhosis.[14,19] These results highlight the potential of this combination as a next-generation regimen capable of addressing current treatment limitations.

To gain deeper insight into the within-host dynamics of HCV suppression under BEM and RZR combination therapy, we used a mechanistic multiscale model developed previously.[20–23] Originally applied to model the viral kinetics in HCV patients treated with daclatasvir, an NS5A inhibitor or telaprevir, an HCV protease inhibitor,[20] and later to patients treated with danoprevir,[22] an NS3/4A protease inhibitor, or to combinations of three different DAAs,[24] this model provided critical information by distinguishing the suppression of intracellular HCV RNA production from the inhibition of virus assembly and secretion from an infected cell and captured the characteristic triphasic decline in HCV RNA levels following treatment initiation. Building on this foundation, we applied a similar multiscale modeling approach to characterize the dynamics of HCV decline in patients treated with the BEM/RZR combination. Our goal was to quantify drug effectiveness, identify treatment response phases, and inform optimal treatment durations. Specifically, we evaluated more than 200 individuals, both cirrhotic and non-cirrhotic, infected with HCV GT 1 through 4, enabling a comprehensive quantitative assessment of treatment response across diverse clinical subgroups.

METHODS

Clinical data

In the phase II clinical trial (Clinicaltrials.gov NCT05904470[18]), a total of 275 patients were enrolled and received 550 mg BEM and 180 mg RZR once daily for 8 weeks. Eligible participants were adults aged 18–85 years with chronic HCV infection who were DAA-naïve and had no cirrhosis (F0–F3) or compensated cirrhosis (F4). Further details about the clinical trial can be found in references.[18,25]

Of the 275 trial participants, 215 were classified as treatment-adherent based on pill counts and plasma drug levels and constituted the population we focused on for analysis.[12,19] Of the treatment-adherent population, 46.5% were male, with mean age 51 years, and 72.6% were White (**Table 1**). The majority (70.2%) were infected with GT 1 (151/215), followed by GT 3 (58/215; 27.0%), GT 2 (4/215; 1.9%), and GT 4 (2/215 = 0.9%). The treatment-adherent cohort predominantly comprised non-cirrhotic patients (F0–F3; 84.2%, 181/215), distributed across fibrosis stages as follows: F0 (49/215, 22.8%), F1 (60/215, 27.9%), F2 (51/215, 23.7%), and F3 (21/215, 9.8%). Patients with compensated cirrhosis (F4) accounted for 15.8% (34/215) of the cohort. In each fibrosis stage, GT 1 made the majority with ~60 to 85%, followed by GT 3 with ~15 to 35%, while GT 2 and 4 were less than 5% represented.[12,19]

Overall, SVR12 rates (i.e., the fraction of individuals with undetectable VL at 12 weeks after the end of treatment) were high, reaching 98% (210/215). SVR12 was higher among patients without cirrhosis (F0–F3; 99%, 180/181) compared to those with compensated cirrhosis (F4; 88%, 30/34).[12,19]

Ethics statement

The current study is not a clinical trial and only involved re-analyses of the previously collected de-identified data and was deemed not human subjects research by the Los Alamos National Laboratory Institutional Review Board.

Multiscale modeling

To analyze the antiviral effect of the fixed-dose BEM/RZR combination (BEM/RZR), we employed a multiscale model we previously developed and used to model the effects of HCV polymerase, protease, and NS5A inhibitors administered singly or in combination.[20–24]

The multiscale model extends the standard target-cell-limited model,[26,27] which includes uninfected target cells (T), infected cells (I), and free virus (V), by incorporating key processes involved in intracellular HCV RNA (R) replication and virion assembly and secretion (**Figure 1**). The model also includes an equation for the dynamics of alanine aminotransferase (ALT) as it provides additional information for estimating the parameter δ, the rate of infected cell death. Details about

Table 1 Baseline characteristics of the per-protocol treatment-adherent population and treatment response as proportion of patients achieving SVR12 according to HCV genotype and cirrhosis

Per-protocol treatment-adherent ($n = 215$)	
Mean age, year (range)	51 (20–85)
Male sex, *n*	100 (46.5%)
Genotype	*n*
1	151 (70.2%)
2	4 (1.9%)
3	58 (27.0%)
4	2 (0.9%)
Fibrosis	
F0	49 (22.8%)
F1	60 (27.9%)
F2	51 (23.7%)
F3	21 (9.8%)
F0–F3	181 (84.2%)
F4	34 (15.8%)
Race	
Asian	44 (20.5%)
Caucasian	156 (72.6%)
Black/African American	6 (2.8%)
Other	9 (4.2%)
SVR12	210/215 (97.7%)
F0–F3	180/181 (99.5%)
GT 1	121/122 (99.2%)
GT 3	53/53 (100.0%)
F4	30/34 (88.2%)
GT 1	26/29 (89.7%)
GT 3	4/5 (80.0%)

the mathematical formulation of the multiscale model are given in S1_Text. As shown in **Figure** 1 the possible modes of action of BEM/RZR are represented by four intracellular parameters: ε_α, which denotes the effectiveness of the drug in reducing the HCV RNA production rate; ε_s, which represents the effectiveness of the drug in inhibiting virus assembly and secretion; κ, the factor by which drug therapy enhances the degradation rate of HCV RNA; and γ, representing the drug-induced enhancement of the degradation of HCV replication templates, (e.g., replication complexes or negative strand HCV RNA), thereby inhibiting HCV RNA production. The parameters ε_α and ε_s are constrained between 0 and 1, where 0 indicates no drug effect and 1 indicates 100% efficacy in blocking the corresponding intracellular process. The parameter κ is assumed to be ≥ 1 and $\gamma \geq 0$.

The four potential modes of action are supported by the following. BEM is a modified guanosine nucleotide prodrug inhibitor of the HCV NS5B polymerase. It is metabolized intracellularly into an active 5'triphosphate metabolite, which inhibits NS5B-dependent HCV replication by incorporating into the nascent HCV RNA, leading to chain termination. RZR is an HCV NS5A inhibitor and drugs in this class were found to act by both blocking HCV replication and an early step in virion assembly.[20,28] While we know of no direct experimental evidence that BEM or RZR increase the degradation rate of intracellular HCV RNA, fitting models to clinical data has suggested this is a possible mode of action.[20,29] Further, another HCV drug, IFN-α, has been shown to increase the degradation rate of HCV RNA at high concentrations *in vitro*.[30] Lastly, a number of HCV models and one *in vitro* experiment have explored the possibility of drug-induced enhancement of HCV replication template degradation, thereby inhibiting HCV RNA production.[21,22,29–31]

Model parameter estimation

We simultaneously fit the $\log_{10} V(t)$ and $\log_{10} A(t)$ derived from the analytic solutions to the logs of the VL and ALT data, respectively, using a mixed-effects approach as implemented in Monolix R2024R1 (Lixoft, Antony France). We statistically compared the quality of the model fits using the corrected Bayesian Information Criterion (BICc). 95% confidence intervals (CI_{95}) of model parameters were calculated with Monolix 2024R1. For the best-fitting model, we also conducted model validation including residual plots and visual predictive checks (**Figure** S1). The parameters $\alpha_R = 40$ viral RNA copies/d, $\rho = 8.18$/d and $\mu = 1$/d were fixed based on previous studies.[20,23] All remaining model parameters including the initial VL and initial level of ALT were estimated from the data.

Covariates for HCV genotypes and fibrosis stages

Our main study focus was to evaluate a set of categorical covariates that reflect discrete differences between clinically relevant patient subgroups across GT 1–4 and fibrosis groups F0 to F4. We distinguished patients with cirrhosis (F4) from those without (F0–F3), based on the clinical relevance of cirrhosis as a major determinant of disease progression, prognosis, and treatment response. Analyses were further stratified by HCV GT, with comparisons performed between GT 1 and 3. GT 2 and 4 were excluded due to insufficient sample sizes for meaningful analysis.

Statistical significance of covariates was calculated using the Wald-test implemented in Monolix R2024R1.

Predicting virologic response rates from viral kinetics data

We evaluated the time required to go below the LLOQ, defined as ≤15 IU/mL HCV RNA, as this threshold strongly correlates with SVR, indicative of long-term viral clearance and low risk of relapse.[32]

Virologic response was assessed at early timepoints to evaluate treatment effectiveness. Very rapid virologic response (vRVR) was defined as HCV RNA ≤ LLOQ at day 7, and rapid virologic response (RVR) as HCV RNA ≤ LLOQ at week 4. For each response definition, the proportion of patients achieving vRVR and RVR was calculated along with their respective CI_{95}.

RESULTS

BEM/RZR with multiple modes of action

To characterize the antiviral effects of the BEM/RZR combination, eqs (2) and (4) (from S1_Text) were fitted to longitudinal HCV RNA and ALT data from 215 per-protocol, treatment-adherent patients simultaneously. Multiple candidate model structures were evaluated to represent different mechanisms of drug action. We also assessed whether inclusion of fibrosis stage or HCV GT as covariates improved the model fit by incorporating them into parameters governing inhibition of HCV RNA production (ε_α), inhibition of virion assembly and secretion (ε_s), intracellular RNA degradation (κ), decay of the HCV replication complex (γ), and infected cell loss (δ) (S1_Text).

We first evaluated the primary antiviral mechanisms by including inhibition of HCV RNA production (ε_α) and virion assembly/secretion (ε_s). This dual-mechanism model (M5) provided a better fit than single-mechanism models, as indicated by a lower BICc (507; **Table 2** and **Table S1**), supporting combined effects on viral production and assembly.

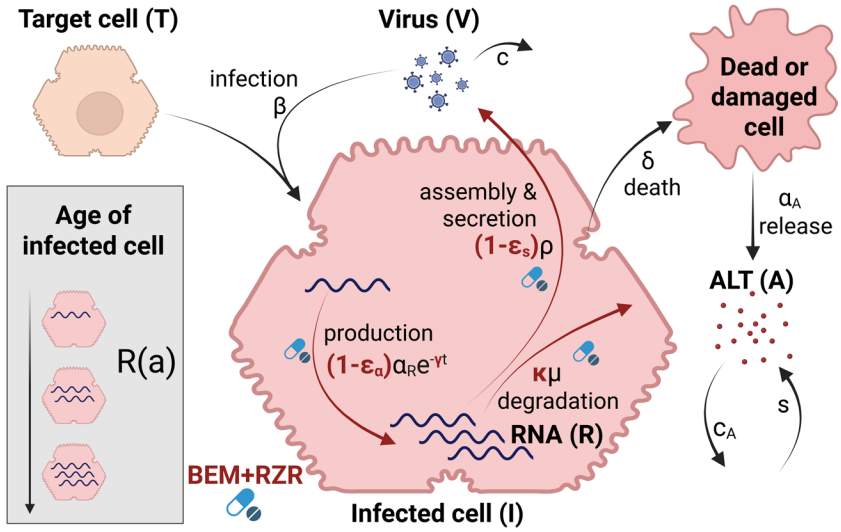

Figure 1 Schematic illustration of the multiscale model. The model describes the dynamics of target cells (T), infected cells (I), virus (v), and ALT (A). Target cells are infected by virus V according to the law of mass-action with rate constant β. The model keeps track of the time since a cell has been infected, denoted as the age (a) of the infected cell. As a function of a, the amount of intracellular positive-strand viral RNA (R) changes as it is produced at the maximum rate α_R. degrades at rate μ, and is assembled into virions at rate ρ. Virus is assumed to be cleared by a first-order process at rate c. The DAAs are modeled as potentially having multiple modes of action: inhibition of the intracellular production of viral RNA (ε_α), inhibition of virus assembly and release (ε_s), an increase in the degradation rate of positive-strand viral RNA by a factor κ, and a decrease in the rate of positive strand HCV RNA production (γ), possibly due to degradation of replication complexes, or equivalently negative-strand viral RNAs, that serve as the template for positive-strand HCV RNA synthesis. ALT has a background production rate s and it is cleared at per capita rate c_A. An amount of ALT α_A is released when an infected cell dies at rate δ. Created in BioRender. Zitzmann, C. (2026) https://BioRender.com/glfp.

We next examined whether additional mechanisms improved model performance. Allowing enhanced intracellular RNA degradation ($\kappa > 1$) yielded the lowest -LL (365), indicating the best likelihood-based fit. However, this improvement was offset by increased model complexity, that is the model having more free parameters, resulting in a higher BICc (515; ΔBICc = +8). Further inclusion of replication complex decay ($\gamma > 0$) increased the BICc to 534 (ΔBICc = +27). Thus, despite improved likelihood, these additional mechanisms were not supported when accounting for model complexity.

Drug efficacy depends on the fibrosis stage

We next evaluated GT and fibrosis stage as covariates on ε_α, ε_s, κ, and γ (**Tables S2–S7**), capturing variation across HCV GTs (GT1–GT4) and fibrosis stages (F0–F4). Fibrosis was also examined using clinically relevant groupings: mild vs. advanced fibrosis (F0–F2 vs. F3–F4) and non-cirrhotic vs. cirrhotic disease (F0–F3 vs. F4).

Incorporation of GT as a covariate did not improve model performance, suggesting no detectable GT-dependent differences in antiviral activity within the modeled parameters (**Table S2**). Similarly, modeling fibrosis as four individual stages (F0–F4) was not supported due to increased model complexity, despite achieving one of the lowest likelihood values (−LL = 338; model F53, Table S3), which was offset by a high BICc (565).

Rather than modeling each fibrosis stage separately, grouping patients into categories provides a more clinically meaningful classification and introduces fewer additional parameters. Progression from F3 to F4 reflects the development of cirrhosis, a qualitative transition marked by architectural remodeling, impaired hepatic function, and increased risk of clinical complications. Thus, to better capture these transitions, two categorical fibrosis groupings were explored: mild vs. advanced fibrosis (F0–F2 vs. F3–F4) and non-cirrhotic vs. cirrhotic disease (F0–F3 vs. F4) (**Tables S4** and **S5**). The cirrhosis-based grouping outperformed the fibrosis-based grouping and was therefore selected as the final model, given its clinical relevance and established role in guiding treatment decisions and prognostic assessment.[33]

The overall best-performing model according to BICc incorporated fibrosis group (F0–F3 vs. F4) as a categorical covariate on ε_α and ε_s, estimated $\kappa > 1$, and has γ fixed to 0 (**Table 2**, model B24 in **Table S5**). Despite the additional parameters, this model achieved the lowest BICc (498), representing a 9-point improvement over the simple model with two modes of action above without covariates (BICc = 507). In this model, the efficacy constant in inhibiting HCV RNA production (ε_α) was estimated at 0.9859 [CI_{95}: 0.9814–0.9894] in non-cirrhotic patients (F0–F3) and 0.9935 [CI_{95}: 0.9880–0.9965] in patients with cirrhosis (F4), with a statistically significant covariate effect ($P = 0.0091$; **Table 3**). Similarly, the efficacy constant in inhibiting virion assembly and secretion (ε_s) was estimated at 0.9978 [CI_{95}: 0.9970–0.9984] in non-cirrhotic patients and 0.9904 [CI_{95}: 0.9812–0.9952] in cirrhotic patients, and while this was a small difference it was highly significant ($P = 2.4 \times 10^{-5}$). The drug-induced enhancement in the HCV RNA degradation rate (κ) was estimated at 1.70 [CI_{95}: 1.52–1.96], corresponding to a 70% increase in the intracellular HCV RNA degradation rate. This model provided an excellent description of the data and accurately reproduced the rapid early decline in HCV RNA, with mean reductions of 1.4 $\log_{10}$, 2.9 $\log_{10}$, and 3.3 $\log_{10}$ at 6, 12, and

Table 2 Single and multiple modes of action models with and without covariates for fibrosis stage group

Single and multiple modes of action models without covariates

Model	Drug effectiveness in inhibiting HCV RNA production (ε_α)	Drug effectiveness in inhibiting virion assembly and secretion (ε_s)	Drug-induced enhancement in HCV RNA degradation by factor (κ)	Drug-induced enhancement in HCV replication complex degradation (γ)	Loss rate of infected cells (δ) (/day)	-LL	BICc
M1	0.9996 [0.9995, 0.9997]	0	1	0	3.345 [0.308–0.386]	937	1,060
M2	0	1 [0.9999, 1]	1	0	0.354 [0.323–0.388]	594	717
M5	0.9874 [0.9846, 0.9897]	0.9986 [0.9982, 0.9989]	1	0	0.265 [0.242–0.291]	371	507
M11	0.9877 [0.9835, 0.9909]	0.9978 [0.9971, 0.9983]	1.387 [1.032, 5.487]	0	0.271 [0.232–0.316]	365	515
M15	0.9858 [0.9818, 0.989]	0.9974 [0.9962, 0.9982]	1.794 [1.53, 2.188]	0.02753 [0.0173, 0.04382]	0.240 [0.213–0.270]	371	534

Single and multiple modes of action models with and without covariates for fibrosis stage group with γ = 0

Model	Drug effectiveness in inhibiting HCV RNA production (ε_α)	Drug effectiveness in inhibiting virion assembly and secretion (ε_s)	Drug-induced enhancement in HCV RNA degradation factor (κ)	Loss rate of infected cells (δ) (/day)	-LL	BICc
B6	F0–F3 = 0.9869 [0.9816, 0.9907] F4 = 0.9932 [0.9901, 0.9954] (*P* = 0.00158)	F0–F3 = 0.9989 [0.9985, 0.9992] F4 = 0.9955 [0.9926, 0.9973] (*P* = 1.91e-06)	1	0.254 [0.232–0.278]	353	500
B24	F0–F3 = 0.9859 [0.9814, 0.9894] F4 = 0.9935 [0.988, 0.9965] (*P* = 0.00913)	F0–F3 = 0.9978 [0.997, 0.9984] F4 = 0.9904 [0.9812, 0.9952] (*P* = 2.44e-05)	1.705 [1.516, 1.963]	0.269 [0.245–0.296]	338	498
D24.1	F0–F3 = 0.984 [0.9793, 0.9877] F4 = 0.9945 [0.9905, 0.9969] (P = 0.000584)	F0–F3 = 0.9976 [0.9963, 0.9984] F4 = 0.9902 [0.9809, 0.9950] (*P* = 3.34e-05)	1.847 [1.476, 2.501]	F0–F3 = 0.290 [0.263, 0.320] F4 = 0.230 [0.184, 0.286] (*P* = 0.0526)	342	508

95% confidence intervals in [], **P*-values are based on Wald-test.

24 hours after treatment initiation, following a pharmacological delay of ~2 hours (**Figure** 2a,b).

Analysis of the full viral kinetics revealed a characteristic triphasic decline in HCV RNA following treatment initiation (**Figure** 2c). The first phase was dominated by rapid clearance of free virions from plasma, with an estimated clearance rate of c = 19.6/day, corresponding to a virion half-life of ~51 minutes. The second phase reflected the combined effects of intracellular HCV RNA degradation and loss of infected hepatocytes, governed by κμ + δ = 1.97/day ($t_{1/2}$ = 8.4 h). Intracellular HCV RNA decayed at a rate κμ = 1.70/day ($t_{1/2}$ = 9.8 h), while infected cells were cleared at a rate δ = 0.269/day ($t_{1/2}$ = 2.6 days). The third and slowest phase represented clearance of HCV replication complexes or negative-strand RNA in conjunction with infected cell loss and is described by γ + δ. As no drug-induced effect on γ was identified (γ = 0), the third-phase kinetics were driven entirely by infected cell loss.

We also tested estimating the plasma viral clearance rate (c) independently for each GT and fibrosis group (i.e., using covariates on this parameter) and found it remained consistent across groups (**Table S1**).

GT 1 and GT 3 patients exhibited similar second-phase half-lives (~8.3 h; κμ + δ), primarily driven by rapid intracellular HCV RNA degradation (κμ). Although first- and second-phase viral declines were comparable between GTs, the infected-cell loss rate was slightly higher in GT 3 (δ = 0.30/day) than in GT 1 (δ = 0.26/day) (**Figure** 3), resulting in a statistically significantly faster overall decline in GT 3 (*P* = 0.0021; **Figure** 2e). Analyses were limited to GT 1 and GT 3, which comprised the majority of participants, whereas GT 2 and GT 4 included only six patients.

When stratified by fibrosis stage, first- and second-phase kinetics were similar between groups, with half-lives of 51 minutes (viral clearance rate, *c*) and 8.4 hours (κμ + δ), respectively. However, the first-phase decline lasted ~2 hours longer in patients with F0–F3 than in those with F4 (D_1^{F0-F3} = 8.4 h vs. D_1^{F4} = 6.5 h) leading to a 3 log first phase decline in VL for patients with F0–F3 vs. a 2.3 log decline for patients with cirrhosis (F4). Conversely, the second-phase decline was ~10 hours longer in F4 compared with F0–F3 (D_2^{F0-F3} = 36 h vs. D_2^{F4} = 46 h) implying that the VL dropped an additional 1.3 logs during the second phase in F0–F3 patients vs. an additional 1.6 logs in F4 patients. As in the GT analysis, third-phase dynamics were driven by infected-cell loss, with estimated half-lives of 2.5 days in F0–F3 and 2.7 days in F4, which were not significantly different statistically (*P* = 0.23; **Figure** 3), but which over the 8-week treatment time yielded noticeably less viral decline (**Figure** 2d).

Table 3 Estimated population parameters

Symbol	Description	Unit	Fixed effects (RSE%)	95% CI
V_0	Baseline HCV RNA	IU/mL	6.48 (0.79)	6.37–6.57
δ	Loss of infected cells	1/day	0.27 (4.90)	0.24–0.30
α_R	HCV RNA production	1/day	40	Fixed
ρ	Virion assembly and secretion	1/day	8.18	Fixed
c	HCV clearance	1/day	19.62 (4.90)	17.95–21.45
μ	HCV RNA degradation	1/day	1	Fixed
τ_v	Pharmacologic delay	Hours	1.8 (4.82)	1.6–1.9
s	ALT secretion	IU/L	5.23 (3.46)	4.88–5.59
c_A	ALT clearance	1/day	0.30 (4.29)	0.28–0.33
A_0	Baseline ALT	U/L	31.57 (5.68)	28.26–35.28
Modes of action				
ε_α	Drug effectiveness in inhibiting production in fibrosis stage groups F0–F3 vs. F4		F0–F3: 0.9859 (0.21) F4: 0.9935 (0.22) *P*-value = 0.00913*	F0–F3:0.9814–0.9894 F4: 0.9880–0.9965
ε_s	Drug effectiveness in inhibiting virion assembly and secretion in fibrosis stage groups F0–F3 vs. F4		F0–F3: 0.9978 (0.04) F4: 0.9904 (0.37) *P*-value = 2.4×10^{-5}*	F0–F3: 0.9970–0.9984 F4: 0.9812–0.9952
κ	Drug-induced enhancement in HCV RNA degradation		1.70 (6.70)	1.52–1.96
γ	Drug-induced decrease in HCV RNA production rate by factor $e^{-\gamma t}$	1/day	0	

Fixed-effect estimates are reported with relative standard errors (RSE%). The values of α_R, ρ, and μ were fixed according to.[20,23]
**P*-values are based on Wald-test.

Overall, long-term viral clearance in the model is driven by the loss of infected hepatocytes (δ). GT-specific differences in individual model parameters were observed between GT 1 and GT 3 in parameters related to virion assembly/secretion (ε_s), intracellular RNA degradation (κ), and infected-cell loss. The inclusion of GT as a covariate did not improve the model fit and covariate effects were not significant (**Table S2**). In contrast, although significant differences in ε_α and ε_s were detected between fibrosis stages (F0–F3 vs. F4), infected-cell loss rates were similar across these groups (**Figure 3**), suggesting that fibrosis-related differences in viral decay are more likely attributable to variations in antiviral effectiveness rather than differences in infected hepatocyte loss.

Predicted time to undetectable HCV RNA levels

Time to undetectable HCV RNA, defined as HCV RNA at or below the LLOQ, was evaluated given its strong association with sustained viral clearance and a low risk of relapse. In addition, we examined the time to reach a more stringent theoretical cure threshold corresponding to ~10 viral particles distributed within 15 liters of extracellular fluid, equivalent to an HCV RNA concentration of 6.67×10^{-4} IU/mL. This threshold, called a "cure boundary"[33] provides a conceptual definition of viral eradication. Using a threshold of 10 virions may be an underestimate as not all viral particles are infectious, and even if some residual virions are infectious, they may be controlled and cleared by the host immune response.[33]

The median time for HCV RNA to decline below the LLOQ is ~11.4 days (**Figure 4a**), with the cure boundary achieved after about 6.6 weeks of treatment. Clear differences were observed between GTs. Patients infected with GT 1 showed the slowest viral decline, reaching undetectable HCV RNA levels after a median of 13.0 days and achieving the cure boundary after 7.0 weeks. In contrast, patients with GT 3 infection (58/215) exhibited the most rapid response, reaching undetectable levels after a median of 8.6 days (compared to GT 1: $P = 0.00024$, *t*-test) (**Figure 4b**) and reaching the cure boundary after 5.6 weeks (compared to GT 1: $P = 0.0062$, *t*-test).

Differences were also observed when results were stratified by cirrhosis status. Non-cirrhotic patients (F0–F3) and patients with cirrhosis (F4) required median times of 11.0 and 15.6 days ($P = 0.0035$, *t*-test), respectively, to reach undetectable HCV RNA levels (**Figure 4c**). The median time to cure was estimated to be 6.5 weeks in non-cirrhotic patients and 6.9 weeks in cirrhotic patients ($P = 0.32$, *t*-test).

Simulating the viral declines in all patients using their estimated specific parameters further showed that a very rapid virologic response (vRVR), defined as achieving undetectable HCV RNA within the first week of treatment, occurred in 26.5% [CI_{95}: 21.1–32.8%] of patients overall (57/215), and in 37.9% [CI_{95}: 26.6–50.8%] of patients infected with GT 3 (22/58). In contrast, a rapid virologic response (RVR), defined as undetectable HCV RNA by week 4, was achieved in 95.3% [CI_{95}: 91.7–97.5%] of patients overall (205/215), including all patients with GT 3 infection and 82.4% [CI_{95}: 66.5–91.7%] of patients with compensated cirrhosis (F4; 28/34). Importantly, regardless of GT or fibrosis stage, all patients except one patient with cirrhosis achieved HCV RNA levels at or below the LLOQ by week 6 of treatment (**Figures 4b,c**).

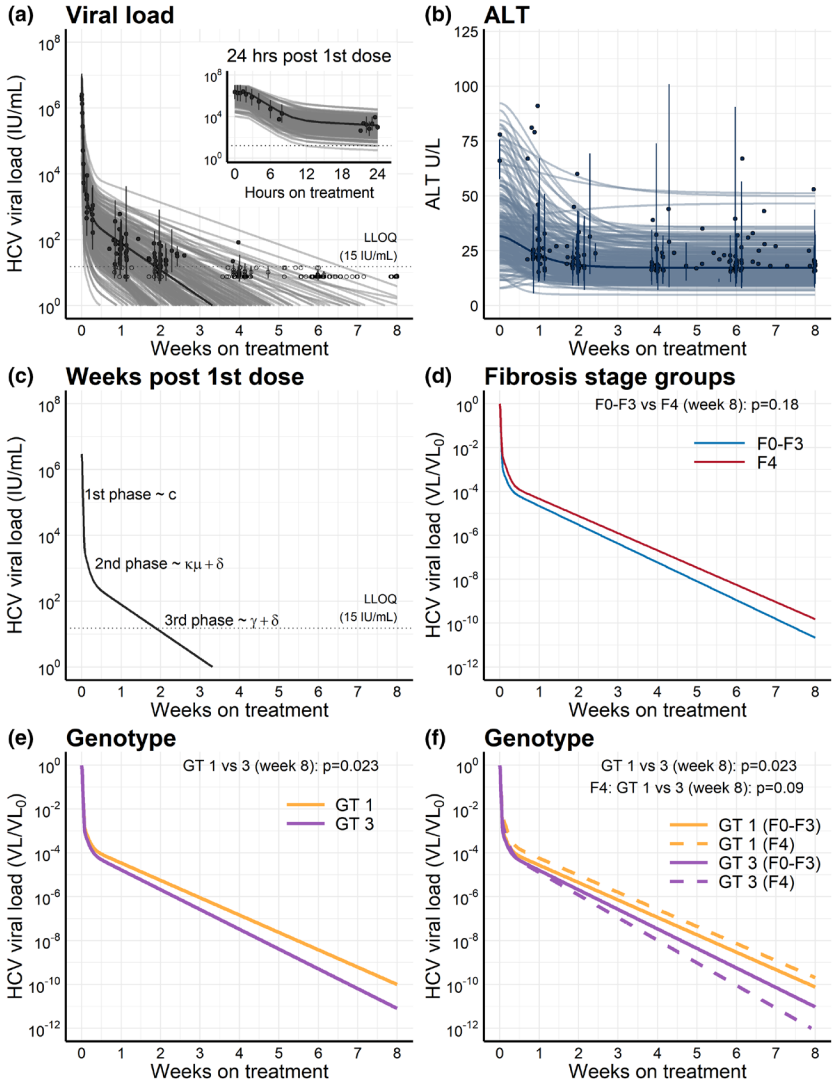

Figure 2 HCV RNA and ALT decline during treatment with BEM and RZR (Model B24, see S1_Text and S2_Text). (**a**) HCV RNA decline. The lower limit of quantification (LLOQ) is 15 IU/mL (dotted horizontal line). Black dots indicate observed values above the LLOQ; open circles represent measurements below the LLOQ. (**b**) ALT levels following treatment initiation based on the best-fitting model. (**c**) Long-term triphasic decline of HCV RNA post-treatment initiation. (**d**) HCV RNA decline relative to baseline stratified by fibrosis stage groups (F0–F3 vs. F4), (**e**) Comparison of viral load decline relative to baseline for genotypes 1 and 3, and (**f**) Comparison of viral load decline relative to baseline for genotypes 1 and 3 and by fibrosis stage groups (F0–F3 vs. F4).

DISCUSSION

DAAs have changed the paradigm of HCV treatment by significantly shortening therapy duration, typically to 8–12 weeks, and achieving SVR rates exceeding 95%. Despite these advances, treatment gaps persist. In the United States, ~2.4 million people are living with HCV, yet only about 120,000 individuals initiate treatment annually, falling short of the estimated 260,000 treatments per year needed to meet national elimination goals.[34] Barriers contributing to this gap include limited access to health care, high treatment costs, treatment adherence, and hard-to-treat patient subgroups, such as individuals infected with GT 3 and/or compensated cirrhosis.

BEM and RZR constitute a novel combination of DAAs that demonstrated high antiviral efficacy in a phase II clinical trial.[12–14] BEM, a nucleotide analog inhibitor of the HCV NS5B RNA-dependent RNA polymerase, exerts potent suppression of viral RNA synthesis.[15] RZR is a second-generation NS5A inhibitor.[16,17] While the exact role of NS5A inhibitors is unclear, it is believed that they impair both HCV RNA replication and virion assembly and secretion.[35] Compared to earlier DAA regimens, BEM and RZR exhibit enhanced intracellular potency, favorable pharmacokinetic profiles, and pan-genotypic activity.[12–14] These properties support their potential to achieve rapid viral clearance and shorten treatment duration.

To better understand the within-host dynamics of HCV suppression under BEM/RZR therapy and the mechanisms of drug action, we fitted a previously developed multiscale model[20] to longitudinal HCV RNA and ALT data from 215 treatment-adherent patients. Comparison of alternative models showed that accurately capturing patient viral kinetics required inclusion of three

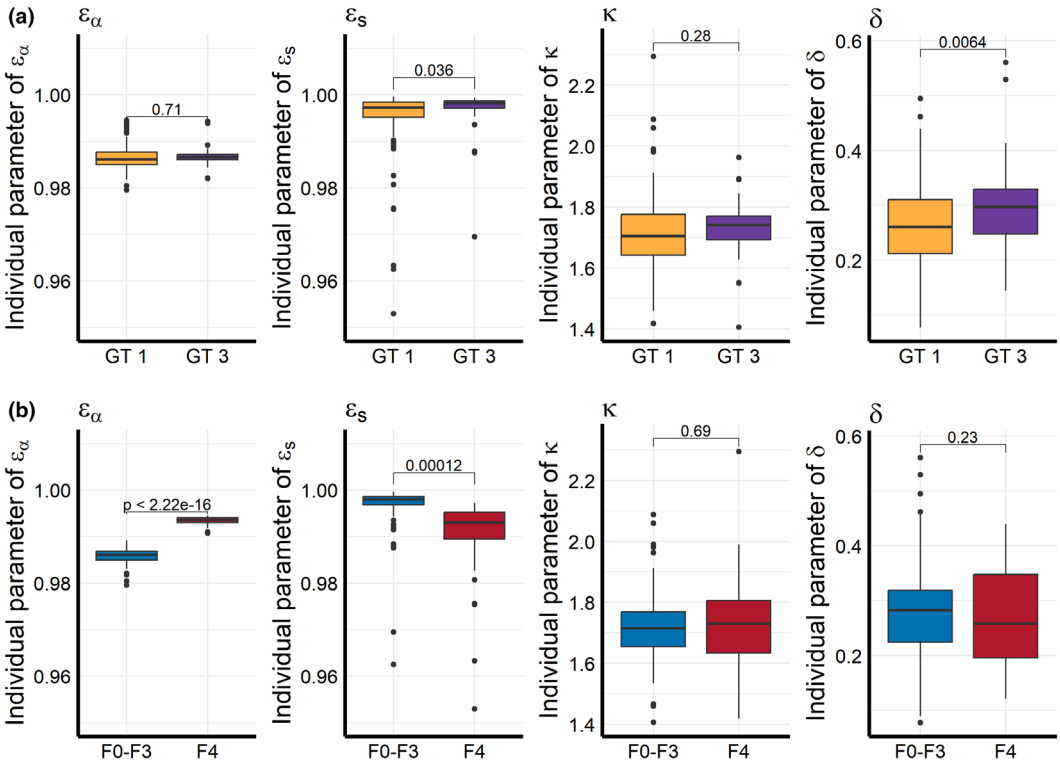

Figure 3 Individual parameter estimates stratified by HCV genotype and fibrosis stage for the best-fitting model, which included fibrosis group as a covariate on ε_α and ε_s, with $\kappa > 1$ and γ fixed to 0. (**a**) Individual parameters for genotypes GT 1 and GT3 and (**b**) grouped fibrosis stages F0–F3 vs. F4 for ε_α (inhibition of viral RNA production), ε_s (inhibition of virus secretion and release), κ (enhancement of HCV RNA degradation) and δ (loss rate of infected cells). *P*-values are based on *t*-tests.

intracellular effects: inhibition of HCV RNA production, inhibition of virion assembly and secretion, and enhanced intracellular HCV RNA degradation. Models assuming a single mechanism were unable to capture either the magnitude or timing of viral decline. Together, these findings suggest that the clinical efficacy of BEM and RZR results from complementary inhibition at multiple stages of the HCV life cycle.

Quantitatively, the best model predicted very high inhibition of intracellular HCV RNA production. Inhibition of RNA replication (ε_α) was estimated at 98.6% in non-cirrhotic patients and 99.4% in cirrhotic patients ($P = 0.009$), while inhibition of HCV virion assembly and secretion (ε_s) exceeded 99% across fibrosis stages. Treatment was also associated with a 70% increase in intracellular HCV RNA degradation ($\kappa = 1.7$/day). Although small fibrosis-associated differences were observed in these efficacy parameters, antiviral activity remained uniformly high, demonstrating consistent BEM and RZR potency in advanced liver disease.

The model closely reproduced the rapid early antiviral response observed clinically, with mean declines of 1.4 $\log_{10}$, 2.9 $\log_{10}$, and 3.3 $\log_{10}$ HCV RNA at 6, 12, and 24 hours following treatment initiation, after a short pharmacological delay of ~2 hours. These early dynamics are clinically relevant and reflect early, drug-driven viral suppression associated with sustained clearance and low relapse risk. An important strength of this modeling framework is its ability to capture the characteristic triphasic decline in HCV RNA under BEM/RZR therapy. The first phase reflects rapid clearance of free virus from plasma, the second phase represents the combined effects of intracellular HCV RNA degradation and loss of infected hepatocytes, while the third phase is driven primarily by infected cell clearance. The presence of a distinct phase reflecting intracellular degradation of HCV RNA, which is absent in simpler extracellular models, underscores the importance of explicitly accounting for intracellular viral processes when evaluating potent DAA combinations.

From a clinical perspective, the selected model predicts rapid viral suppression across all patient subgroups. Median time to undetectable HCV RNA was ~11 days overall, 8.6 days in GT 3-infected patients, and 15.6 days in patients with cirrhosis (F4). Time to reach the cure boundary remained short even in historically harder-to-treat populations, at ~5.6 weeks for GT 3 and 6.9 weeks for F4. Importantly, all patients achieved undetectable HCV RNA levels by week 6 of therapy except for one patient with cirrhosis. These results indicate that early viral suppression is predominantly drug-driven and largely independent of GT or fibrosis stage.

There are limitations of this study. The biochemical mechanisms mediating the inhibition of viral assembly/secretion and the enhanced degradation of HCV RNA are not known. Also, we have no in vitro data confirming these mechanisms of action. Second, we assumed constant efficacy and did not include explicit pharmacokinetics/pharmacodynamics. This is a common approach in many viral dynamics studies.[21–24,26,27,33,36–39] Finally, we did not include an explicit immune response, which would make the model more complex, and for which we do not have commensurate

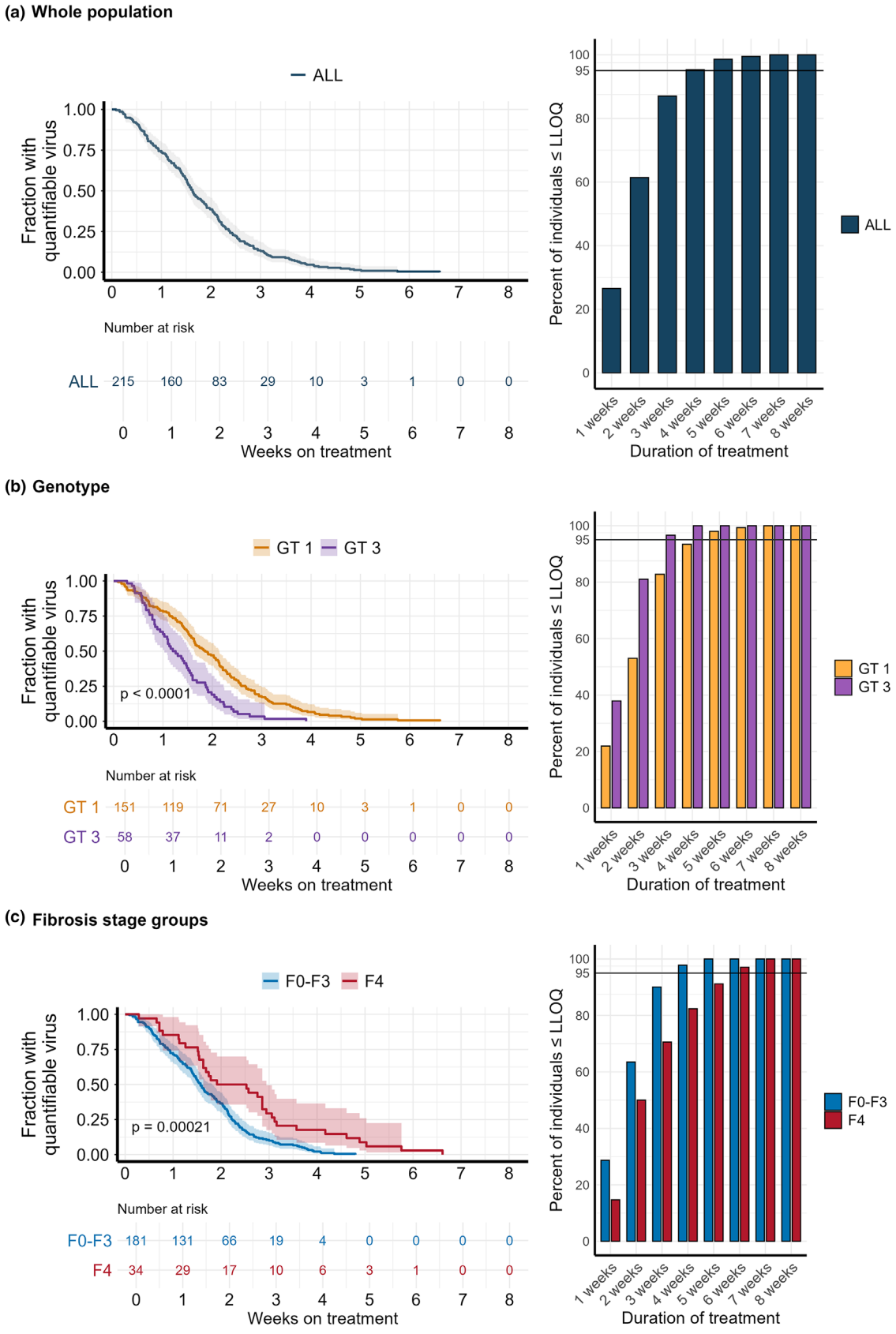

Figure 4 Time-to-undetectable HCV RNA. Time-to-undetectable HCV RNA (≤15 IU/mL) analyses for (**a**) all patients, (**b**) genotypes GT 1 and 3, and (**c**) fibrosis stage group F0–F3 and F4. Kaplan–Meier plot of time to undetectable HCV RNA, with numbers at risk shown below (left). P-values were calculated using the log-rank test. Percentage of individuals achieving undetectable HCV RNA (right).

data. However, the death of infected cells is mostly due to immune elimination as the virus is not known to be cytopathic. Thus, our parameter δ implicitly includes immune effects.

In summary, BEM/RZR achieves high antiviral activity by simultaneously inhibiting HCV RNA production, HCV virion assembly and secretion, and enhancing intracellular HCV RNA degradation, leading to rapid and durable viral clearance even in GT 3-infected and cirrhotic patients. This mechanistic understanding provides a strong biological rationale for the high clinical cure rates observed and supports future efforts to optimize or potentially shorten treatment duration without compromising efficacy.

SUPPORTING INFORMATION

Supplementary information accompanies this paper on the *Clinical Pharmacology & Therapeutics* website (www.cpt-journal.com).

ACKNOWLEDGMENT

The authors acknowledge the use of ChatGPT (OpenAI, GPT-5.2) to assist with grammar, readability, and organization of selected manuscript sections. All generated text was reviewed, revised, and approved by the authors. The AI tool did not contribute to study design, data analysis, interpretation of results, or development of figures and tables.

FUNDING

Partial funding for this work was provided by the National Institutes of Health (R01 AI116868 and R01 AI078881). Portions of this work were done under the auspices of the U.S. Department of Energy under contract 89233218CNA000001 and supported by contract NFE-00165 from Atea Pharmaceuticals.

CONFLICT OF INTEREST

X-J. Zhou is an employee of Atea Pharmaceuticals. Carolin Zitzmann, Ruy Ribeiro, Aurelien Marc, and Alan Perelson were partially funded by a subcontract from Atea Pharmaceuticals to Los Alamos National Laboratory.

AUTHOR CONTRIBUTIONS

C.Z., R.M.R. and A.S.P. wrote the manuscript; R.M.R. and A.S.P. designed the research; C.Z., R.M.R., A.M., X.J.Z. and A.S.P. performed the research; C.Z., R.M.R. and A.S.P. analyzed the data.

1. Dietz, C. & Maasoumy, B. Direct-acting antiviral agents for hepatitis C virus infection—from drug discovery to successful implementation in clinical practice. *Viruses* **14**, 1325 (2022).
2. Afdhal, N. *et al*. Ledipasvir and sofosbuvir for untreated HCV genotype 1 infection. *N. Engl. J. Med.* **370**, 1889–1898 (2014).
3. Fried, M.W. Side effects of therapy of hepatitis C and their management. *Hepatology* **36**(5 I), s237–s244 (2002).
4. Heim, M.H. 25 years of interferon-based treatment of chronic hepatitis C: an epoch coming to an end. *Nat. Rev. Immunol.* **13**, 535–542 (2013).
5. Dusheiko, G. & Free, R. Side effects of α interferon in chronic hepatitis C. *Hepatology* **26**(S3), 112S–121S (1997).
6. Sagnelli, E. *et al*. Resistance detection and re-treatment options in hepatitis C virus-related chronic liver diseases after DAA-treatment failure. *Infection* **46**, 761–783 (2018).
7. Sarrazin, C. Treatment failure with DAA therapy: importance of resistance. *J. Hepatol.* **74**, 1472–1482 (2021).
8. Chen, W.M. *et al*. High viral load predicts virologic failure in chronic genotype 2 hepatitis C virus-infected patients receiving glecaprevir/pibrentasvir therapy. *J. Formos. Med. Assoc.* **119**, 1593–1600 (2020).
9. Chan, A., Patel, K. & Naggie, S. Genotype 3 infection–the last stand of hepatitis C virus. *Drugs* **77**, 131–144 (2017).
10. Martin, M.T. & Deming, P. Closing the gap: the challenges of treating hepatitis C virus genotype 3 infection. *Pharmacotherapy* **37**, 735–747 (2017).
11. Zhou, X.J. *et al*. Clinical evaluation of potential interaction between bemnifosbuvir and ruzasvir with an assessment of food effect: results of a phase 1 study in healthy participants. *Clin. Pharmacol. Drug Dev.* **14**, 461–471 (2025).
12. Jucov, A. *et al*. Abst. TOP-251 efficacy and safety of Bemnifosbuvir and Ruzasvir after 8 weeks of treatment in patients with chronic hepatitis C virus (HCV) infection. *J. Hepatol.* **82**, S851 (2025).
13. Good, S.S., Luo, S., Lin, K., Vo, A., Agrawal, N.G.B. & Sommadossi, J.P. Bemnifosbuvir and ruzasvir in combination exhibit potent synergistic antiviral activity in vitro while maintaining a favorable nonclinical safety profile in vivo. *Antiviral Res.* **237**, 106137 (2025).
14. Jucov, A. *et al*. Abst. THU-382 Lead-in cohort results from a phase 2 study of a novel 8-week combination regimen of Bemnifosbuvir and Ruzasvir in patients with chronic hepatitis C virus infection. *J. Hepatol.* **80**, S819 (2024).
15. Zhou, X.J. *et al*. Bemnifosbuvir (BEM, AT-527), a novel nucleotide analogue inhibitor of the hepatitis C virus NS5B polymerase. *Expert Opin. Investig. Drugs* **33**, 9–17 (2024).
16. Asante-Appiah, E. *et al*. In vitro antiviral profile of ruzasvir, a potent and pangenotype inhibitor of hepatitis C virus NS5A. *Antimicrob. Agents Chemother.* **62**, e01280-18 (2018).
17. Tong, L. *et al*. Discovery of ruzasvir (MK-8408): a potent, pan-genotype HCV NS5A inhibitor with optimized activity against common resistance-associated polymorphisms. *J. Med. Chem.* **60**, 290–306 (2017).
18. Berliba, E. *et al*. Safety, pharmacokinetics, and antiviral activity of AT-527, a novel purine nucleotide prodrug, in hepatitis C virus-infected subjects with or without cirrhosis. *Antimicrob. Agents Chemother.* **63**, e01201–19 (2019). https://doi.org/10.1128/aac.01201-19.
19. Jucov, A. Efficacy and safety of bemnifosbuvir and ruzasvir after 8 weeks of treatment in patients with chronic hepatitis C virus (HCV) infection. *EASL 2025 May 7–10 Amsterdam*. Poster.
20. Guedj, J. *et al*. Modeling shows that the NS5A inhibitor daclatasvir has two modes of action and yields a shorter estimate of the hepatitis C virus half-life. *Proc. Natl. Acad. Sci. USA* **110**, 3991–3996 (2013).
21. Rong, L. & Perelson, A.S. Mathematical analysis of multiscale models for hepatitis C virus dynamics under therapy with direct-acting antiviral agents. *Math. Biosci.* **245**, 22–30 (2013).
22. Rong, L. *et al*. Analysis of hepatitis C virus decline during treatment with the protease inhibitor danoprevir using a multiscale model. *PLoS Comput. Biol.* **9**, e1002959 (2013).
23. Cardozo, E.F. *et al*. Disentangling the life-spans of hepatitis C virus infected cells and intracellular vRNA replication-complexes during direct acting antiviral therapy. *J. Viral Hepat.* **27**, 261–269 (2019).
24. Lau, G. *et al*. Efficacy and safety of 3-week response-guided triple direct-acting antiviral therapy for chronic hepatitis C infection: a phase 2, open-label, proof-of-concept study. *Lancet Gastroenterol. Hepatol.* **1**, 97–104 (2016).
25. Zitzmann, C. *et al*. Abst. 0089 multiscale modeling of results from a phase 2 study of an 8-week combination regimen of Bemnifosbuvir and ruzasvir in patients with chronic hepatitis C virus infection. The liver meeting: 2025 abstracts. *Hepatology* **82**(S1), S85–S86 (2025).

26. Neumann, A.U. *et al*. Hepatitis C viral dynamics in vivo and the antiviral efficacy of interferon-alpha therapy. *Science* **282**, 103–107 (1998).
27. Perelson, A.S. & Ke, R. Mechanistic modeling of SARS-CoV-2 and other infectious diseases and the effects of therapeutics. *Clin. Pharmacol. Ther.* **109**, 829–840 (2021).
28. McGivern, D.R. *et al*. Kinetic analyses reveal potent and early blockade of hepatitis C virus assembly by NS5A inhibitors. *Gastroenterology* **147**, 453–462.e7 (2014).
29. Zitzmann, C., Ribeiro, R.M., Marc, A., Zhou, X.J. & Perelson, A.S. Bemnifosbuvir: an HCV NS5B inhibitor with multiple modes of action. *Clin. Pharmacol. Ther.* **120**, 552–562 (2026).
30. Dahari, H., Sainz, B. Jr., Perelson, A.S. & Uprichard, S.L. Modeling subgenomic hepatitis C virus RNA kinetics during treatment with alpha interferon. *J. Virol.* **83**, 6383–6390 (2009).
31. Goyal, A. *et al*. Modeling predicts direct-acting antiviral therapy for 5-weeks may cure recent or chronic hepatitis C infection among people with undetectable viral RNA by day 7. *J Infect Dis* (2026). https://doi.org/10.1093/INFDIS/JIAG260.
32. Pawlotsky, J.M. *et al*. EASL recommendations on treatment of hepatitis C: final update of the series q European Association for the Study of the liver*. *J. Hepatol.* **73**, 1170–1218 (2020).
33. Perelson, A.S. & Guedj, J. Modelling hepatitis C therapy—predicting effects of treatment. *Nat. Rev. Gastroenterol. Hepatol.* **12**, 437–445 (2015).
34. CDC. *Too Few People Treated for Hepatitis C | VitalSigns* (CDC). https://www.cdc.gov/vitalsigns/hepc-treatment/index.html?utm_source=chatgpt.com. Accessed June 16, 2025.
35. Scheel, T.K.H. & Rice, C.M. Understanding the hepatitis C virus life cycle paves the way for highly effective therapies. *Nat. Med.* **19**, 837–849 (2013).
36. Perelson, A.S., Neumann, A.U., Markowitz, M., Leonard, J.M. & Ho, D.D. HIV-1 dynamics in vivo: virion clearance rate, infected cell life-span, and viral generation time. *Science (1979)* **271**, 1582–1586 (1996).
37. Goyal, A. *et al*. Modeling-based response-guided DAA therapy for chronic hepatitis C to identify individuals for shortening treatment duration. *Open Forum Infect. Dis.* **9**, ofac157 (2022). https://doi.org/10.1093/OFID/OFAC157.
38. Gorstein, E. *et al*. Modeling based response guided therapy in subjects with recent hepatitis C infection. *Antiviral Res.* **180**, 104862 (2020).
39. Canini, L. & Perelson, A.S. Viral kinetic modeling: state of the art. *J. Pharmacokinet. Pharmacodyn.* **41**, 431–443 (2014).